

Tuning MPL signaling to influence hematopoietic stem cell differentiation and inhibit essential thrombocythemia progenitors

Lu Cui^a, Ignacio Moraga^{b,c,d,e}, Tristan Lerbs^a, Camille Van Neste^a, Stephan Wilmes^e, Naotaka Tsutsumi^{b,c,d}, Aaron Claudius Trotman-Grant^{b,c,d}, Milica Gakovic^{b,c,d,e}, Sarah Andrews^f, Jason Gotlib^g, Spyros Darmanis^{h,i}, Martin Enge^{h,j}, Stephen Quake^h, Ian S. Hitchcock^f, Jacob Piehler^k, K. Christopher Garcia^{b,c,d,1}, and Gerlinde Wernig^{a,l,1}

^aDepartment of Pathology, Stanford University School of Medicine, Stanford, CA 94305; ^bHHMI, Stanford University School of Medicine, Stanford, CA 94305; ^cDepartment of Molecular and Cellular Physiology, Stanford University School of Medicine, Stanford, CA 94305; ^dDepartment of Structural Biology, Stanford University School of Medicine, Stanford, CA 94305; ^eSchool of Life Sciences, University of Dundee, Dundee DD15EH, United Kingdom; ^fYork Biomedical Research Institute, Department of Biology, University of York, Heslington, YO10 5DD York, United Kingdom; ^gDepartment of Medicine, Division of Hematology, Stanford University School of Medicine, Stanford, CA 94305; ^hDepartment of Bioengineering, School of Bioengineering and Medicine, Stanford University, Stanford, CA 94305; ⁱMicrochemistry, Proteomics, Lipidomics and NGS Department Genentech Inc., South San Francisco, CA, 94080; ^jDepartment of Oncology-Pathology Karolinska Institutet, 171 64 Stockholm, Sweden; ^kDepartment of Biology and Center for Cellular Nanoanalytics (CellNanos), University of Osnabrück, Barbarastrasse 11, 49076 Osnabrück, Germany; and ^lInstitute for Stem Cell Biology and Regenerative Medicine, Stanford University School of Medicine, Stanford, CA 94305

Contributed by K. Christopher Garcia, November 23, 2020 (sent for review August 24, 2020; reviewed by Stefan N. Constantinescu, Andre Larochelle, and Sachdev S. Sidhu)

Thrombopoietin (TPO) and the TPO-receptor (TPO-R, or c-MPL) are essential for hematopoietic stem cell (HSC) maintenance and megakaryocyte differentiation. Agents that can modulate TPO-R signaling are highly desirable for both basic research and clinical utility. We developed a series of surrogate protein ligands for TPO-R, in the form of diabodies (DBs), that homodimerize TPO-R on the cell surface in geometries that are dictated by the DB receptor binding epitope, in effect “tuning” downstream signaling responses. These surrogate ligands exhibit diverse pharmacological properties, inducing graded signaling outputs, from full to partial TPO agonism, thus decoupling the dual functions of TPO/TPO-R. Using single-cell RNA sequencing and HSC self-renewal assays we find that partial agonistic diabodies preserved the stem-like properties of cultured HSCs, but also blocked oncogenic colony formation in essential thrombocythemia (ET) through inverse agonism. Our data suggest that dampening downstream TPO signaling is a powerful approach not only for HSC preservation in culture, but also for inhibiting oncogenic signaling through the TPO-R.

thrombopoietin signaling | megakaryopoiesis | myeloproliferative neoplasm | hematopoietic stem cells

Since the landmark cloning of thrombopoietin (TPO) (1–4) and its receptor MPL (TPO-R) (5–7), there has been interest in characterizing the role of the TPO/TPO-R interaction in normal and pathological hematopoiesis. TPO signaling plays key roles in regulating megakaryopoiesis and platelet production (8, 9) and in the support of hematopoietic stem cell (HSC) maintenance and self-renewal (10–16). Consequently, aberrant TPO/TPO-R signaling can lead to severe hematological disorders, including myeloproliferative neoplasms (MPNs) (17, 18) and bone marrow failure syndromes (19, 20).

Despite initial hurdles with first generation recombinant thrombopoietin, which stimulated autoantibody formation resulting in cytopenia, several second-generation peptide/small-molecule TPO mimetics are now approved for immune thrombocytopenia and hepatitis C-associated thrombocytopenia and bone marrow failure syndromes (21). Side effects of TPO mimetics include thrombocytosis, possibly thrombosis, bone marrow reticulosis, and rebound thrombocytopenia (22). Thus, fine tuning this therapeutically important signaling axis remains an important goal.

TPO is a prototypical four-helix bundle cytokine (23) and engages TPO-R using the canonical “growth hormone” mechanistic and structural paradigm (24, 25). TPO dimerizes TPO-R

and induces downstream signaling through the JAK/STAT pathway, principally activating JAK2 and STAT5 (26). However, the few studies that have addressed how TPO-R dimerization dynamics and geometry, in response to TPO, relate to signaling output (27), have hinted that TPO-R signaling could be manipulated in therapeutically useful ways that are not exhibited by the natural TPO ligand. This is important given that the activities of the natural TPO molecule are clinically limited (28). Although synthetic small molecule TPO-R agonists have been developed (23), as well as agonist antibodies (29), they appear to phenocopy

Significance

TPO is a cytokine that signals through the receptor MPL (or TPO-R), and is essential for megakaryocyte differentiation and maintenance of hematopoietic stem cells (HSCs). TPO signaling is deregulated in essential thrombocythemia (ET). Here, we engineered diabodies (DBs) against the TPO-R ECD as surrogate TPO ligands to manipulate TPO-R signaling, from full to partial agonism, and that show decoupling of the dual functions of TPO/TPO-R (i.e., HSC maintenance versus megakaryopoiesis). We subsequently discovered that partial agonistic DBs, by reducing the strength of the TPO-R signal, not only preserved HSCs in culture, but also blocked oncogenic signaling in ET. This finding has the potential to improve HSC cultures for transplants, as well as serve as a unique therapeutic approach for ET.

Author contributions: K.C.G. and G.W. designed research; L.C., I.M., T.L., C.V.N., S.W., N.T., M.G., S.A., M.E., I.S.H., J.P., and G.W. performed research; J.G., S.Q., and K.C.G. contributed new reagents/analytic tools; L.C., I.M., S.D., and G.W. analyzed data; L.C., I.M., A.C.T.-G., I.S.H., J.P., K.C.G., and G.W. wrote the paper; A.C.T.-G. reviewed and edited manuscript; J.G. provided resources; S.D. and M.E. performed library preparation and single-cell RNA sequencing; and K.C.G. and G.W. provided resources and supervision of research.

Reviewers: S.N.C., Université Catholique de Louvain; A.L., National Heart, Lung, and Blood Institute, NIH; and S.S.S., the Donnelly Centre, University of Toronto.

The authors declare no competing interest.

This open access article is distributed under [Creative Commons Attribution-NonCommercial-NoDerivatives License 4.0 \(CC BY-NC-ND\)](https://creativecommons.org/licenses/by-nc-nd/4.0/).

¹To whom correspondence may be addressed. Email: kcgarcia@stanford.edu or gwernig@stanford.edu.

This article contains supporting information online at <https://www.pnas.org/lookup/suppl/doi:10.1073/pnas.2017849118/-DCSupplemental>.

Published December 31, 2020.

TPO-induced signaling and lack the element of fine control of agonist output.

Two particularly relevant studies have hinted at the potential promise of diversifying TPO pharmacology. In one study, the authors showed that artificial chimeric TPO-R fusion proteins, when forced into different symmetrical dimeric receptor orientations, differentially promoted megakaryocyte differentiation, cell adhesion, and myeloproliferative and myelodysplasia phenotypes *in vivo* (27). This intriguing result raised the possibility that engineered ligands that could bind to unmodified TPO-R on natural cells and alter dimer geometry, could potentially induce different functional outcomes. Following this observation, we demonstrated that a dimeric antibody format known as diabodies (DBs), had the capacity to bind to different epitopes on the EPO-R, a highly-related class I cytokine receptor, and induce different dimerization geometries, modulating signal strength (30). These DBs elicited a range of signaling pharmacology, from full to partial agonism. Given that TPO-R and EPO-R both form JAK2-associated homodimeric signaling complexes on the cell surface and exhibit highly similar signaling signatures, these studies motivated us to ask whether we could manipulate TPO-R signaling with engineered surrogate ligands.

In the present study, we manipulate TPO-R signal strength, borrowing a strategy commonly used for GPCRs that has been rarely applied to cytokine receptors. We used DBs as “surrogate” TPO-R ligands that bind to different epitopes on the TPO-R extracellular domain (ECD), and as a result, alter the TPO-R interdimer distance and geometry which results in a perturbed, and fine-tuned, TPO-R downstream signal. We evaluated the activities of these TPO-R DBs by measuring the level of TPO-R dimerization and signaling downstream and exploring their effects on HSC gene expression and differentiation. We also transcriptionally single-cell profiled the effects the DBs and TPO had on proliferation and differentiation of fluorescence activated cell sorting (FACS)-purified human HSCs after *ex vivo* expansion (31, 32). In addition, the cytokine TPO is required in all cell culture media to expand HSCs *ex vivo* for cell therapy (33). Therefore, we evaluated whether substituting TPO with our surrogate agonist TPO-R DBs could influence cell-fate decisions and increase the HSC number for allogeneic HSC transplantation. Several of the partial agonist TPO-R DB molecules control HSC maintenance versus differentiation under *ex vivo* expansion and differentiation conditions, thus pointing to tuning of TPO-R signal strength as a major determinant of HSC homeostasis. Collectively these studies show that DBs can split the dual function of TPO/TPO-R (megakaryopoiesis and HSC maintenance) and that the calibration and tuning of TPO-R can exert differential effects on HSC fate decisions.

Results

Diabodies Induce Different Degrees of Agonistic Activity. As a proxy for the natural TPO ligand, we used DBs, which have highly engineerable scaffolds and the capacity to dimerize their targets because they contain two binding sites. DBs are a dimeric, bivalent antibody format generated through a tandem arrangement of two single-chain variable fragments (scFvs) connected by a short linker. This format results in a dimeric molecule in which the binding sites are closer together and more rigidly connected than a typical IgG-like antibody where two Fabs are linked by an Fc. The closer proximity of the two binding sites in the DBs increases chances for productive TPO-R dimerization and signaling. Previously, a full agonist DB against TPO-R was reported, showing that a DB can in principle dimerize TPO-R in a productive signaling geometry (29). We generated three versions of DBs using sequences of anti-TPO-R DBs, as described in *SI Appendix, Supplementary Materials and Methods* (29, 30, 32). Each of these DBs has different sequences of complementary determining regions (CDR) loops, and therefore likely bind to

different epitopes on TPO-R, thus dimerizing TPO-R in different geometries. Using yeast surface display of the TPO-R D1D2 domains, we found that AK111 appears to bind to an overlapping epitope where TPO binds, and can block TPO binding to 100%. AK119, on the other hand, appears to bind to a partially overlapping epitope with TPO and AK111, and therefore TPO and AK111 can only block AK119 binding by 50% (*SI Appendix, Fig. S1 A and B*).

We then evaluated binding of the three DBs AK111, 113, and 119 to the TPO-R receptor ectodomain (SD1-2) displayed on the surface of yeast, and found that all DBs bound with comparable efficiencies to TPO-R (Fig. 1A), with DBs AK113 and AK111 binding having higher affinity. We next explored whether these DBs were functional in inducing TPO-R signaling. Stimulation of Ba/F3-MPL cells with TPO or the respective DBs induced different levels of TPO-R receptor phosphorylation, with AK119 comparable to TPO, AK113 slightly less than AK119, and AK111 being the least active (Fig. 1B). Upon TPO stimulation, TPO-R is phosphorylated at various tyrosine residues on its intracellular domain. To better understand the signaling properties of the different DBs and distinguish between complete and partial agonistic activity, we investigated the levels of receptor phosphorylation in three stable cell lines expressing TPO-R mutants where Tyr residues (all of which are phosphorylated upon TPO binding) were replaced with Phe (Y591F, Y625F, and Y630F) (Fig. 1C). While Y591F has been shown to be a negative regulator of TPO signaling and dispensable for proliferation (34), Y625F is essential for it. Only the Y625F mutant was seemingly more phosphorylated by AK119 than by AK113 (both higher than TPO). In contrast, phosphorylation was disrupted after AK111 treatment in all mutant cells, suggesting partial agonism. Similarly, AK113 exhibited partial agonistic activities with a lesser phospho-TPO-R:TPO-R ratio than TPO or AK119 in wild-type TPO-R, but less in mutated TPO-R (Fig. 1D). DBs AK119 and 113 show very similar responses to TPO. Indeed, a positive response is shown using doses in the nano-micromolar concentration range, whereas DB AK119 presents a very strong response within picomolar doses. Response saturation is very similar between DB AK 119 and TPO while saturation is observed with lower doses for DB AK111 and 113 (Fig. 1E). This qualitative trend was further confirmed when we studied STAT5 phosphorylation (Fig. 1F) and cell proliferation (Fig. 1G) induced by the three DBs in UT-7 TPO-R cells.

Diabodies Induce Graded Signaling Strengths. TPO not only induces the activation of STAT5/STAT3/STAT1 but, in addition, it activates non-STAT pathways such as the MAPK and PI3K that further modify TPO-mediated responses (Fig. 1H). Previously we showed for EPO-R that alterations on the ligand–receptor binding topology could lead to biased signaling (30), thus we asked whether the same principle would apply to the TPO-R system, and whether TPO-R DBs were engaging these pathways as well. To test this, UT-7 TPO-R cells were stimulated with saturating concentrations of TPO or the three TPO-R DBs for the indicated times and the levels of over 133 molecules were analyzed via phospho-specific antibodies and flow cytometry. We detected activation of 33 different signaling molecules by TPO and the DBs (Fig. 1H). These molecules included members of the STAT family (STAT1, STAT3, and STAT5), MAP kinase family (MEK, p38), and PI3K family (AKT, RSK1, and RPS6). In contrast to the generally monotonic reduction in phosphorylated signaling proteins by the partial agonists (35), we also found activation of important self-renewal switch pathways c-MYC and FOS and survival pathways. This may be a result of the reduction of certain negative regulators resulting in enhanced expression of certain pathways; however, the origins and physiological relevance is not known. Overall, in agreement with our previous results, the activities of the three DBs ranged from

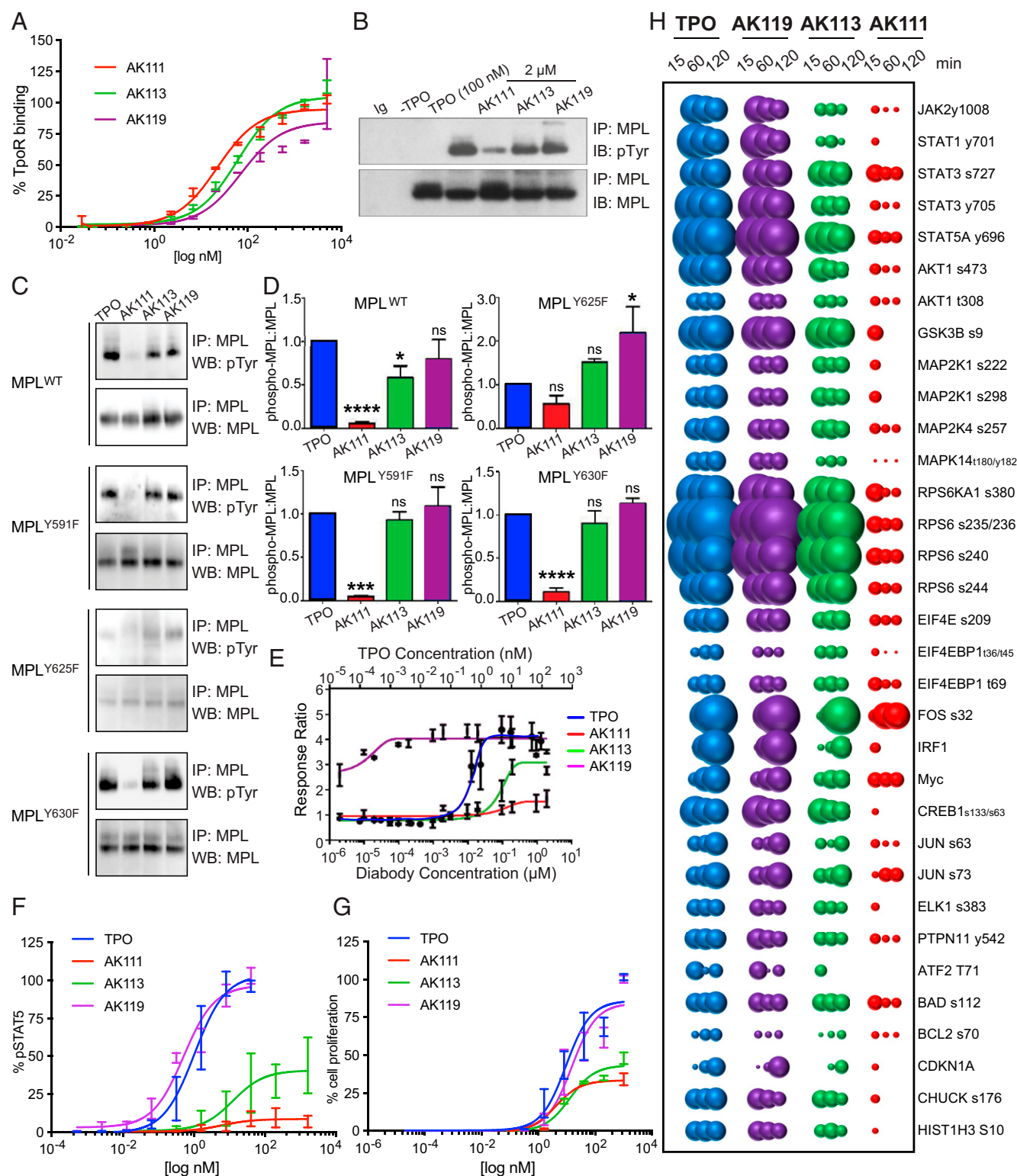


Fig. 1. Diabodies induce different degrees of agonism activity. (A) Levels of TPO-R (MPL) binding in yeast (data are from triplicates mean \pm SD) and (B) levels of MPL phosphorylation promoted by DBs at the indicated dosages in Ba/F3 MPL cells. (C) Study of the level of phosphorylation promoted by different DBs in different phospho mutants of MPL. Y625 corresponds to Y626 in the Uniprot sequence system. (D) Ratio between the nonphosphorylated and phosphorylated MPL forms induced by different DBs in Ba/F3 MPL mutant cells (D and E). Data are from triplicates mean \pm SD, by one-way ANOVA with Dunnett's multiple comparisons test: ns, nonsignificant, * P < 0.05, *** P < 0.001; **** P < 0.0001. (E) Response ratio between low dose of TPO with high dose of TPO and DBs. Data are from triplicates mean \pm SD. (F) Phospho-STAT5 dose-response experiments performed in UT-7 TPO-R cells stimulated with TPO or AK111, AK113, and AK119 for 15 min. Data mean \pm SD are from triplicates. (G) UT-7 TPO-R proliferation in response to TPO or the three DBs for 5 d. (Data mean \pm SD are from triplicates). (H) Diabodies induce graded signaling strengths. Bubble plot representation of the signaling pathways activated by TPO and the DBs at the indicated times in UT-7-TPO-R cells. The size of the bubbles represents the intensity of the signal activated.

full agonism for AK119 to a broad reduction of phosphorylation, indicating partial agonism for AK113 and weak agonism for AK111. Interestingly, not all 33 molecules were activated to the same extent by the DBs (Fig. 1H). When the activation levels induced by the three DBs after 15 min of stimulation were normalized to those induced by TPO, we observed that while TPO and AK119 produced very similar signaling signatures, AK113 elicited a graded response, with some of the pathways more affected than others. For example, AK113 elicited almost full agonism for GSK3B and RPS6 activation but very weak agonism for STAT1 and STAT3 (*SI Appendix*, Fig. S2). Overall our combined signaling data further confirm our previous observations that alterations on the ligand–receptor binding architecture results in fine tuning of the signaling outputs delivered by cytokine receptors.

Diabodies Dimerize TPO-R at the Surface of Living Cells. We asked whether the DB/TPO-R complexes on the cell surface are indeed homodimers or higher-order species resulting from clustering of TPO-R dimers. To test this, we employed dual-color single molecule total internal reflection fluorescence (TIRF) microscopy to quantify dimerization of TPO-R by different DBs in the plasma membrane of living cells. Selective and efficient labeling of TPO-R extracellularly fused to a nonfluorescent, monomeric EGFP (mXFP) was achieved via anti-GFP nanobodies conjugated with Rho11 and Dy647, respectively (Fig. 2A). TPO-R dimerization was quantified by colocalization and cotracking analysis of individual molecules with subdiffractional resolution as schematically depicted in Fig. 2A (Movie S1 and Fig. 2B). In the absence of stimulation, no cotrajectories were observed. Upon addition of TPO or DBs, however, colocalizing TPO-Rs were clearly discerned, though with different efficiencies (Movies S1–S3 and Fig. 2B and C). Relative dimerization levels observed for different DBs are summarized in Fig. 2D. For DB AK119, similar yet slightly increased dimerization as compared to TPO was observed. By contrast, dimerization by DB AK111 and 113 were significantly lower, though above the untreated condition. Since HeLa cells express low levels of JAK2, we coexpressed TPO-R with JAK2 fused to mEGFP (JAK2-mEGFP), which function to increase and stabilize cell-surface levels of TPO-R (36). In JAK2-mEGFP expressing cells, significantly increased TPO-R dimerization by DB AK119 was obtained, similarly to TPO. These higher dimerization levels may be ascribed to productive interactions of JAK2 homomers within the receptor complex. Interestingly, the addition of JAK2-mEGFP did not significantly increase TPO-R dimerization by DB AK111 and 113. This observation suggests that these DBs may form TPO-R dimers with a strongly altered geometry that do not allow such productive interactions between TPO-R-bound JAK2 molecules, which may explain their altered activity profiles.

Diabodies Decouple the Dual Function of TPO/TPO-R during Megakaryocyte Differentiation and Block Oncogenic Signaling through the TPO-R. TPO plays a central role in the differentiation and maturation of megakaryocytes. Thus, we investigated the effects of TPO-R DBs in megakaryocyte differentiation. UT-7 parental cells develop phenotypes similar to megakaryocytes with TPO and to erythrocytes with EPO. To test the effects of DBs in this system, we incubated UT-7 cells with EPO, TPO, or the partial or full agonistic TPO-R DBs for 21 d and then quantified megakaryocytic or erythrocytic differentiation in the cultures. AK113 stimulation resulted in weak up-regulation of megakaryocytic genes and down-regulation of erythroid genes, a physiologic process required during megakaryocytic differentiation (*SI Appendix*, Fig. S3). Next, we analyzed the ability of the three TPO-R DBs to elicit megakaryocyte differentiation in liquid culture of freshly isolated human CD34⁺ hematopoietic stem cell precursors (HSPCs) from bone marrow cells in comparison to TPO. We also isolated megakaryocyte-erythroid progenitors (MEPs) by flow cytometry using the indicated markers

(LIN[−]CD34⁺CD38⁺CD135[−]CD45RA[−]) and assessed colony-forming potential of the three DBs in direct comparison to TPO. We noticed that partial agonists AK111 and AK113 did not support effective megakaryocytic differentiation (Fig. 3A–C) nor colony formation. Despite DBs AK111 and AK113 producing cells expressing megakaryocytic markers CD41 and CD42b, both resulted in significantly decreased numbers of polyploid cells in liquid and semisolid culture conditions and were comparable in their low megakaryocyte differentiation potential to the low stem cell factor (SCF) (20 ng/mL) condition. In contrast, the full agonistic DB AK119 effectively promoted megakaryocytic differentiation and megakaryocytic colony formation to an even greater extent than TPO (Fig. 3A–C). We also noted no significant contribution of TPO DBs to multipotent progenitors (MPPs: lineage-CD34⁺CD38[−]CD90[−]CD45RA[−]), megakaryocyte-erythroid progenitors (MEPs: lineage-CD34⁺CD38⁺CD135[−]CD45RA[−]), and granulocyte-macrophage progenitors (GMPs: lineage-CD34⁺CD38⁺CD135⁺CD45RA⁺), and erythroid precursors, each accounting for <10% of cells both in liquid and semisolid culture conditions (*SI Appendix*, Figs. S4–S6).

Then, we evaluated the differential effects of DBs on HSC propagation and megakaryocytic differentiation when treated with DBs AK111 or 113 or 119 or TPO or low SCF (labeled \emptyset control). We FACS purified single-cell HSPCs and MPPs by their characteristic surface markers (HSC-enriched population: lineage-CD34⁺CD38[−]CD45RA[−]CD90⁺, MPPs: lineage-CD34⁺CD38[−]CD45RA[−]CD90[−]) (Fig. 3D and E) at the indicated time points. In addition to the indicated factors, HSPCs were cultured over 15 d. We discovered that HSPCs cultured without TPO but treated with AK113 or AK111 (partial TPO agonistic DBs) consistently preserved phenotypic HSPCs to a greater extent, 80% and ~50% after 12 d in culture, respectively, compared to only ~10% in conditions treated with TPO or AK119 (full TPO agonistic DB), and very few in \emptyset control (Fig. 3E and F). Through colony forming and serial replating assays, we evaluated the ability of HSPCs to self-renew and form multipotent colonies in vitro after treatment with TPO or DBs AK111, AK113, and AK119 and weekly cell replating over four rounds. Initially, we detected low numbers of CFU-GEMM (colony forming unit that generates myeloid cells) colonies in AK111, AK113, and HSPCs treated with low concentrations of SCF without any additional growth factors or diabodies (\emptyset), compared to twofold increased GEMM colony numbers in TPO-treated HSPCs after one round of replating. After four rounds of replating, however, HSPCs treated with low SCF had low numbers of CFU-GEMM colonies, whereas HSCs treated with TPO or AK119 lost their GEMM colony forming capacity. In a stark contrast, HSPCs treated with DB AK111 and AK113 dramatically increased the number of CFU-GEMM colonies, demonstrating DB AK111 and AK113's ability to enhance HSC stemness exhibited by increased serial replating in vitro (Fig. 3G). In addition to effects on normal HSPCs, we were curious whether partial agonistic DBs could interfere with oncogenic signaling in ET, a myeloid neoplasm, and preleukemic condition with deregulated TPO signaling. Therefore we investigated whether antagonizing TPO signaling would have any therapeutic impact for ET. We assessed ex vivo colony formation from bone marrow samples of patients with ET carrying the MPL^{W515L} or the JAK2^{V617F} mutations. The bone marrow samples were grown without added cytokines or treated with the AK111 DB. We discovered that the AK111 DB not only significantly reduced colony formation in patients with MPLW515L and JAK2V617F mutated ET but also blocked differentiation toward megakaryocytes and platelets (Fig. 3H and I).

Partial Agonistic Diabodies Propagate Hematopoietic Stem Cells In Vitro with Distinct Properties. To get a better understanding of the differential effects of diabodies on gene expression in HSPCs

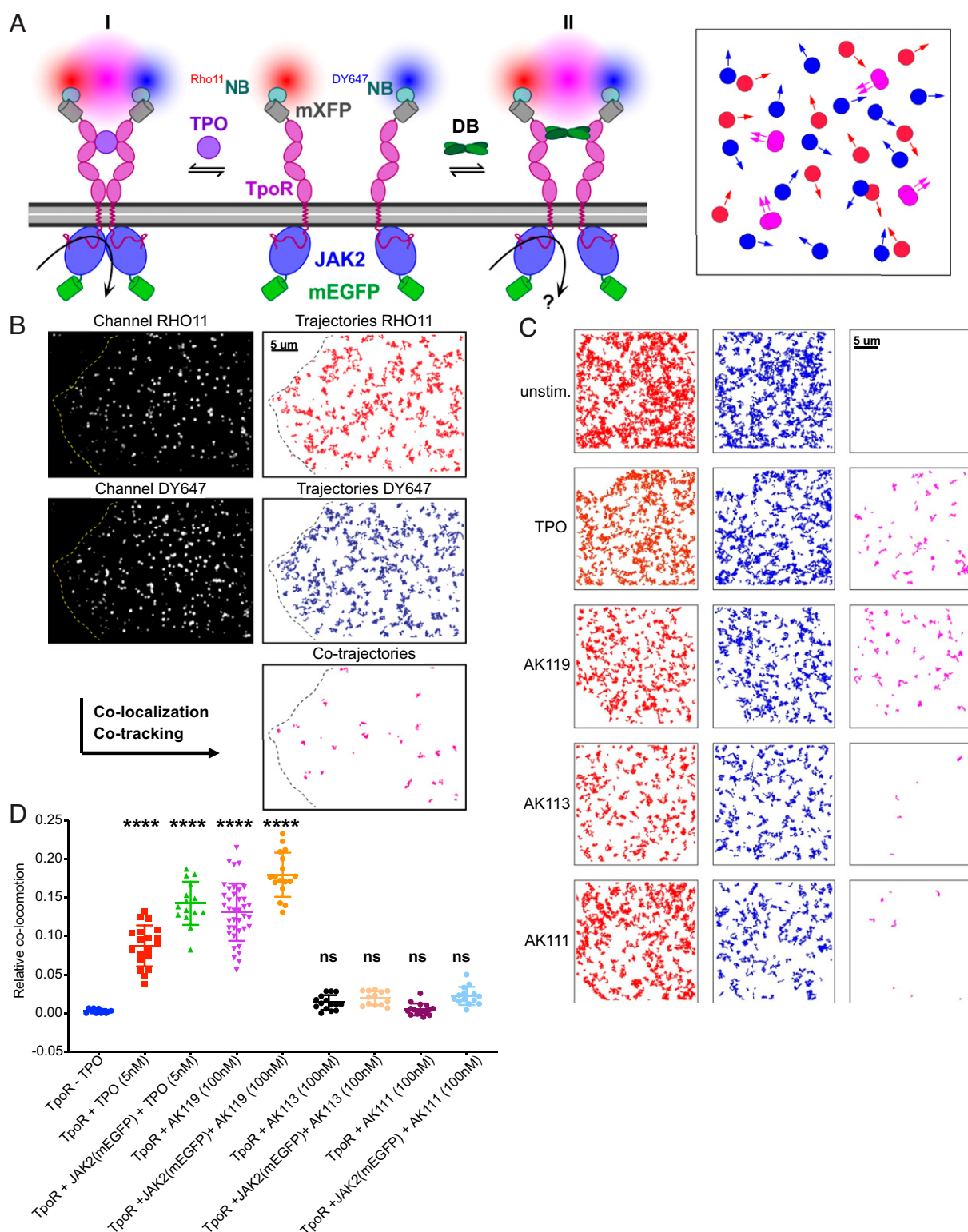


Fig. 2. Diabodies dimerize TPO receptor at the surface of living cells. (A) Cell-surface labeling of TPO-R fused to a nonfluorescent mEGFP (mXFP) using dye-labeled (Rho11 and Dy647) anti-GFP nanobodies (NBs). Coexpression of JAK2-mEGFP can be identified at the single-cell level. Dimerization by TPO (I) and by DBs (II) is quantified by dual-color single-molecule cotracking as schematically depicted on the *Right*. (B) Representative trajectories (from 150 frames acquired in 4.8 s) of individual RHO11-labeled (red) and DY647-labeled (blue) TPO-R and cotrajectories (magenta) observed in a TPO-stimulated cell (cell boundaries are outlined by a dashed line). (Scale bar, 5 μ m.) (C) Trajectories and cotrajectories observed in unstimulated cells and TPO-, AK119-, AK113-, and AK111-treated conditions. (Scale bars, 5 μ m.) (D) Changes in TPO- and DB-induced TPO-R dimerization upon coexpression of JAK2-mEGFP. Each data point represents the relative number of cotrajectories observed in individual cells. Data are expressed as mean \pm SD and analyzed by ordinary one-way ANOVA, **** P < 0.0001; ns, nonsignificant.

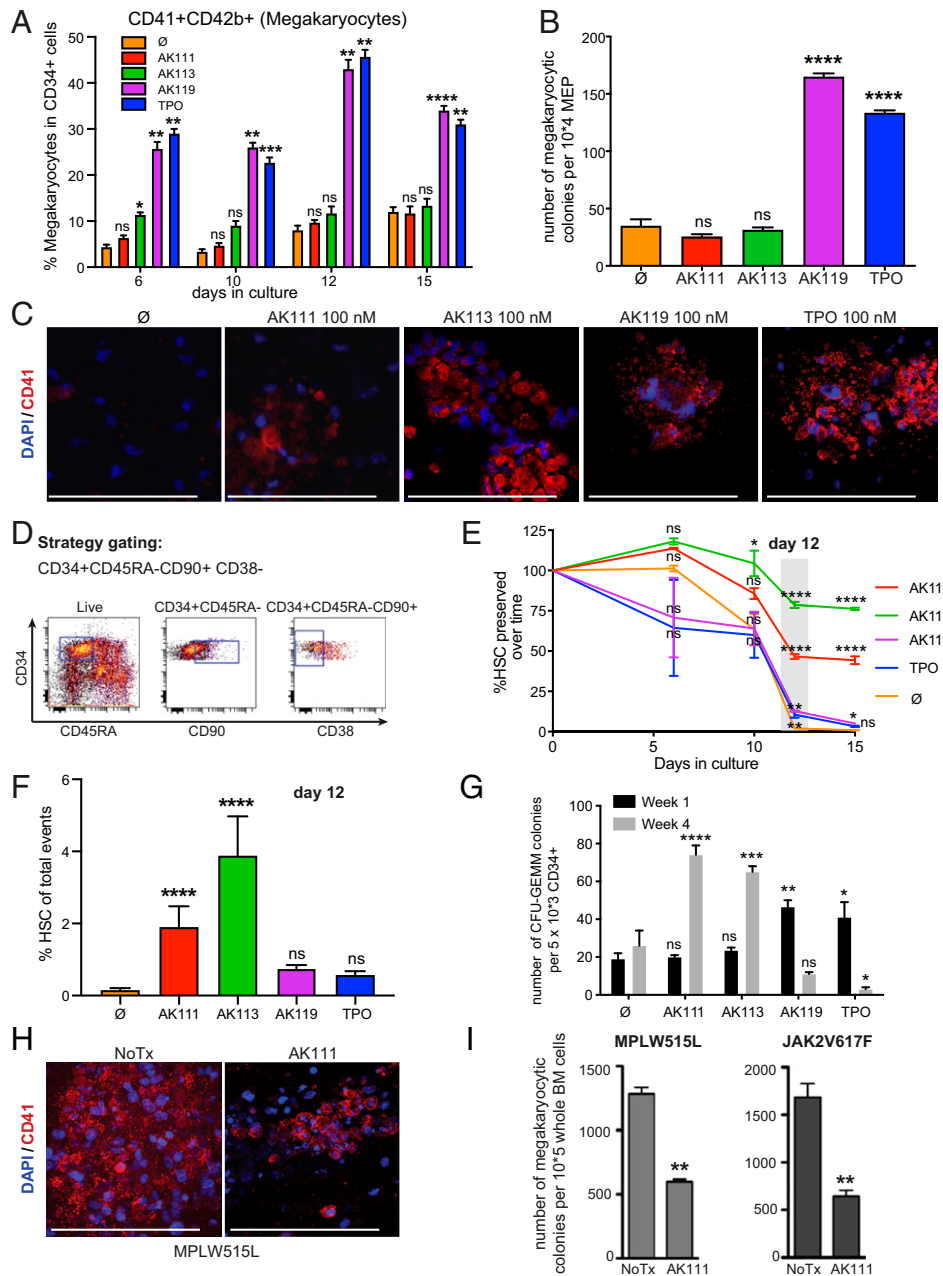


Fig. 3. Diabodies split the dual function of TPO/TPO-R and block oncogenic signaling in essential thrombocythemia. (A) Percentage of megakaryocytes in CD34⁺ cells were quantified over 15 d in culture. Immune phenotypic characterization of liquid cultures of human HSCs (HSCs were sorted as Lin⁻CD34⁺CD45RA⁻CD90⁺CD38⁻ cells on day 0) on indicated days plated under megakaryocytic differentiation-inducing conditions with indicated cytokines or DBs (\emptyset : 20 ng/mL SCF was added to all conditions). Data are expressed as mean \pm SD and analyzed by ordinary two-way ANOVA, * P < 0.05, ** P < 0.01, *** P < 0.001, **** P < 0.0001; ns, nonsignificant. (B) Quantification of MEP-derived colonies in MegaCult cultures demonstrated minimal megakaryocytic differentiation with SCF and partial agonistic DBs AK111 and AK113, and full megakaryocytic differentiation with TPO and full agonistic DB AK119. Data are expressed as mean \pm SD and analyzed by ordinary one-way ANOVA, **** P < 0.0001; ns, nonsignificant. (C) Representative confocal images of MegaCult cultures treated with indicated DBs for 15 d, stained for megakaryocytic markers CD41 (red), and nuclear counterstained with DAPI (blue). (Scale bar, 100 μ m.) (D) Gating strategy for HSC isolation from human donor bone marrow (Live⁺/Lin⁻/CD34⁺CD45RA⁻/CD90⁺CD38⁻). (E) We measured the percent decrease of HSCs at the indicated time points after treatment with \emptyset , AK111, AK113, AK119, or TPO over 15 d. We performed statistical analysis with one-way ANOVA followed by Dunnett's multiple comparisons test with \emptyset as control group. * P < 0.05; ** P < 0.01; **** P < 0.0001; ns, nonsignificant. (F) Percent of HSCs under \emptyset , AK111, AK113, AK119, and TPO induced culture on day 12. Data are expressed as mean \pm SD and analyzed by one-way ANOVA, **** P < 0.0001; ns, nonsignificant. (G) HSCs are harvested and treated for 12 d in liquid culture with the indicated cytokines or partial agonistic DB AK111, AK113, or AK119 were subsequently placed in semisolid methylcellulose culture to evaluate their colony forming capacities over four rounds of weekly replating. Quantification of total numbers of CFU-GEMM colonies at the first and fourth replating for HSCs previously treated with baseline SCF, AK111, AK113, AK119, and TPO in liquid cultures. Data are shown as mean \pm SD. Unpaired t test (** P < 0.01, *** P < 0.001, **** P < 0.0001; ns, nonsignificant). (H) Representative confocal images of collagen-based cultures of MPLW515L mutated bone marrow of patients with essential thrombocythemia immune stained for CD41 (red) and DAPI (blue). (Scale bar, 100 μ m.) (I) Quantification of collagen-based culture assays of MPLW515L and JAK2V617F mutated bone marrow of patients with essential thrombocythemia treated with indicated DB or without (NoTx). Data are shown as mean \pm SD, statistical differences assessed by paired Student's t test (* P < 0.05. ** P < 0.01, *** P < 0.001, **** P < 0.0001).

propagated in culture, we performed single-cell RNA sequencing (scRNA-seq) of HSPCs treated with the DBs which we directly compared to native (=uncultured) HSPCs and MPPs (Fig. 4A). HSPCs are defined as a quiescent stem cell population and maintain only low levels of the cell cycle gene *TP53* (37). We confirmed extremely low expression levels of *TP53* in native uncultured human HSPCs. We observed that HSPCs treated with DB AK111 or AK113 had *TP53* levels even lower than native HSPCs. In contrast, HSPCs cultured solely with TPO or the full TPO agonistic DB AK119 had much higher expression levels of *TP53* (Fig. 4A). We also quantified proliferation by nuclear expression of *MKI67* and found that HSPCs treated with AK111 and AK113 did not proliferate, indicated by their low *MKI67* which was similar to native HSPCs, while HSPCs treated with TPO or AK119 had a much higher *MKI67*, consistent with their active cell proliferation. Compared to native HSPCs, HSPCs cultured with AK111 and AK113 demonstrated similarly low *MKI67* expression (Fig. 4A). This was also the case for *BAX*, an apoptosis regulatory gene; native HSPCs and MPPs were similar to AK111 and AK113 in their low *BAX* expression, which was somewhat higher in HSPCs propagated with TPO or AK119. Uniform manifold approximation and projection (UMAP) analysis of scRNA-seq data of cultured HSPCs revealed 10 subclusters among which three larger groups are discernable. Quite interestingly these data demonstrated that the full agonistic diabody AK119 clustered closely with TPO, while the partial agonistic diabody AK113 clustered in two distinct areas: one area next to TPO and SCF and another area far apart next to AK111. AK111 clustered in a spatially distinct area distant from TPO and AK119 (Fig. 4B). These data support that the different diabodies induce distinct fate decisions in HSPCs.

Next we studied the change in gene expression profile along the differentiation path of HSPCs to megakaryocytes in response to the treatment with different DBs compared to TPO (Fig. 4C and *SI Appendix, Figs. S7 and S8*). Quite comparable to TPO, AK119 activated transcriptional programs in primary HSPCs across the megakaryocyte differentiation spectrum, including *GATA1*, *GATA2*, and *LMO2*, transcriptional programs characteristic for MEP stage, as well as programs pertinent for megakaryocyte precursors and platelets, *TAL1*, *MYBL2*, *VWF*, and *HBD* while inhibiting transcription factors driving myeloid and erythroid differentiation, *CEBPA*, *KIT*, *ANK1*, and *EPOR*. These data are in line with our findings described in Fig. 1, which support that AK119 is a potent and full TPO agonist. Quite in contrast, AK111 appeared to dampen transcriptional activity throughout, only allowing for minimal expression of *GATAs* 1, 2, and selected myeloid transcriptional programs *CEBPA* and *SPI1*. Quite interestingly, AK113 appeared to suppress *MPL* expression in primary cells the most and in a similar manner to that of native uncultured HSCs, which is in line with data we showed earlier demonstrating that it was also the most potent in preserving the undifferentiated stage. In addition, AK113 suppressed megakaryocytic differentiation factors *GATA 1* and *2* to a lesser degree while simultaneously allowing for expression of myeloid instructive programs *KIT* and *SPI1* (Fig. 4C and *SI Appendix, Figs. S7 and S8*). One common feature of all TPO diabodies was the suppression of erythroid differentiation programs (e.g., *ANK1*, *EPOR*, and *ZFPM1* were not expressed), which was quite similar to that of native uncultured HSPCs and MPPs. Thus, the partial agonist DBs show a surprising heterogeneity in induction of gene expression programs which could, in principle, lead to different functional effects.

Partial Agonistic Diabodies Act by Reducing Signal Strength through the TPO/TPO-R. We performed cell clustering of scRNA-seq gene expression data and distinguished three populations labeled as 1, 2, and 3 (Fig. 4D and *SI Appendix, Fig. S9*). Based on their single-cell RNA-seq expression profile, myeloid corresponded to cluster 1,

HSPCs to cluster 2, and megakaryocytic and lineage⁺ to cluster 3. We evaluated the frequencies of these three cell populations treated with partial agonistic DBs in the presence or absence of a TPO-blocking antibody with single-cell RNA sequencing and compared the results to cells treated with SCF or TPO. HSC cultures treated with TPO contained a high percentage of cluster 3, lineage⁺ megakaryocytic cells, which decreased significantly with TPO blocking antibody. As expected, SCF mostly supported myeloid differentiation (cluster 1), while the cells treated with DB AK119 were quite similar to TPO supporting megakaryocytic differentiation (cluster 3). However, unlike TPO, a significant HSPC proportion (cluster 2) was maintained. In general, HSPCs treated with TPO-blocking antibody demonstrated a higher percentage of stem cells (cluster 2) and a lower percentage of megakaryocytic differentiated cells (cluster 3) compared to TPO (which showed the opposite). We observed a similar trend in HSPCs treated with DB AK111 and to a lesser extent with DB AK113, which retains a higher level of signaling activity (*SI Appendix, Fig. S7*). UMAP plots in Fig. 4D demonstrate that treatment with DBs AK111 and with AK113 in a subset of cells appeared to have similar effects to the TPO-blocking antibody on HSPCs after 15 d of in vitro culture. Thus these data suggest that HSPC maintenance/expansion by DBs AK111 and 113 is achieved by inverse agonism of TPO. Collectively these data demonstrate that partially agonizing TPO with DBs can fine tune the switch between HSPC self-renewal and megakaryocytic differentiation and counteract oncogenic signaling in *MPL* and *JAK2* mutated ET (Fig. 4E).

Discussion

Here we have explored the effects of manipulating TPO-R signaling in hematopoietic-fate decisions using surrogate TPO agonists and partial agonistic DBs. We have created a collection of TPO surrogate ligands with graded signaling potencies and strengths, enabling us to study this parameter on HSPC biology. While all three DBs bound with comparable affinities to TPO-R, their downstream signaling outputs greatly differed and determined cell fate—maintenance of an HSPC-like state with DBs AK111 and AK113 versus full maturation to megakaryocytes with AK119. While the structural basis of the differing signaling outputs elicited by the DBs is not resolved here, most likely the DBs bind to different epitopes on the TPO-R, resulting in a different range of dimeric TPO-R orientations and proximities. However, we cannot exclude that other mechanisms are at play, such as that diabodies induce different levels of internalization, degradation/recycling of the TPO-R, which could also influence the signaling properties. This is conceptually consistent with a previous study on DBs to EPO-R that elicited a similar pharmacological profile of full to partial agonism (30, 38). Structural analysis of the DB/EPO-R complexes revealed strikingly different EPO-R dimerization topologies that presumably impacted the orientation of the intracellular signaling machinery. Here we have extended this concept about basic mechanisms of cytokine–receptor signaling, to applications in HSPC biology with therapeutic implications. This study, along with others demonstrating the effects of cytokine partial agonism on cytokine pleiotropy and function in systems such as IL-2, interferons, and stem cell factor, show protein engineering can generate partial agonists with unique pharmacology for dimeric receptors, borrowing conceptually from the GPCR structure–activity approaches, with distinctive functional properties that can be advantageous over wild type (39–41).

Allogeneic HSC transplant is the only curative therapy for numerous hematologic malignancies and autoimmune diseases. While human HSPCs have been successfully purified since the 1980s, their small cell numbers have limited their use in human transplant protocols. Purified HSPC grafts would offer many advantages over CD34⁺-enriched stem cell grafts. For example, purified HSC grafts do not confer acute and chronic graft versus host disease (cGVHD), which is the leading cause of mortality and morbidity following a bone marrow transplant.

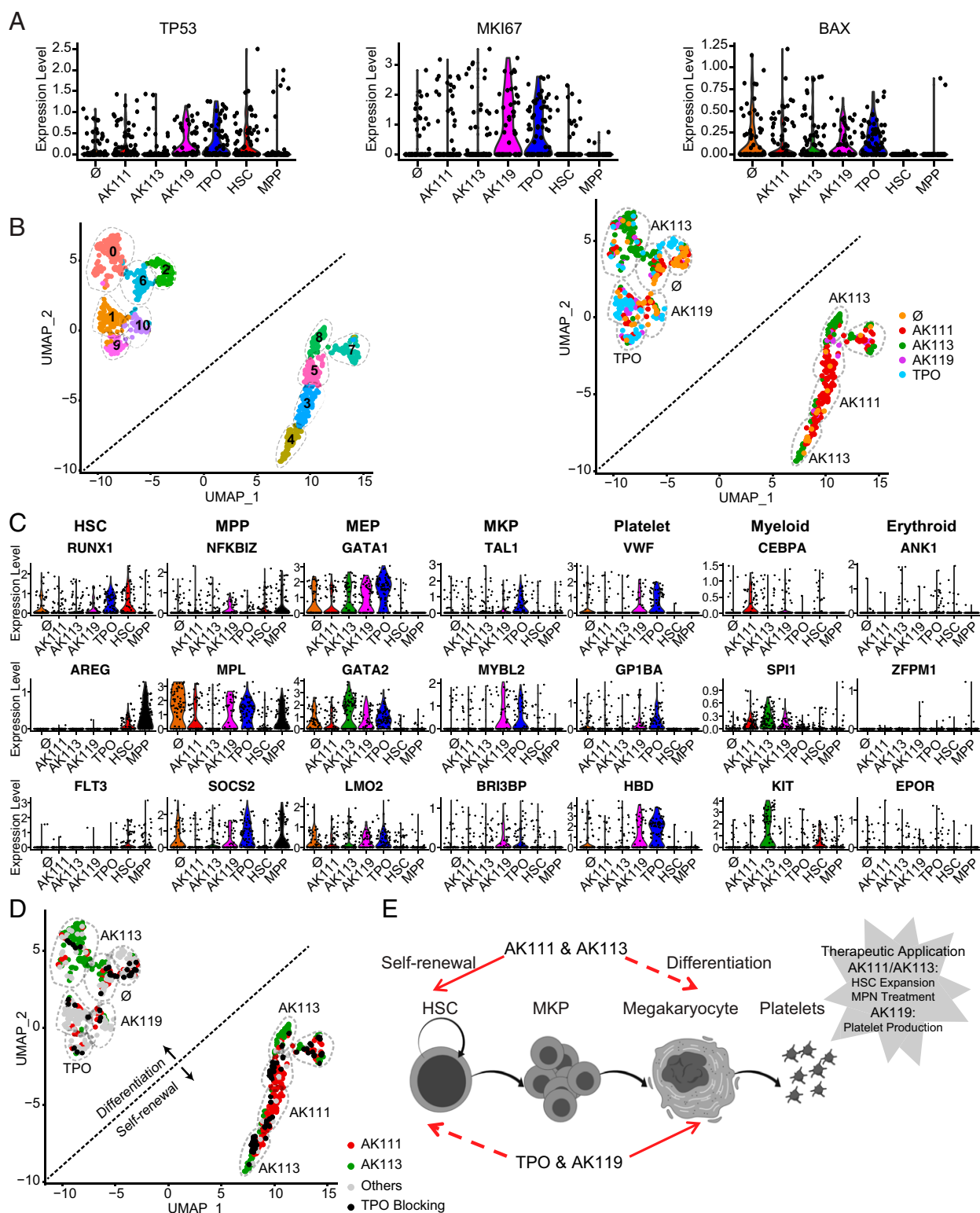


Fig. 4. Partial agonistic diabodies propagate HSCs in vitro with distinct properties. (A) scRNA-seq analysis shows the expression profiles of TP53, MKI67, and BAX (cell proliferation markers) in HSCs after 12-d culture with \emptyset (20 ng/mL SCF) and combined with TPO DBs or TPO (100 nM). (B) UMAP plots showing scRNA-seq data of FACS-isolated human HSCs ($CD34^+CD45RA^-CD90^+CD38^-$) of five different culture conditions: \emptyset (20 ng/mL SCF) and combined with TPO DBs or TPO (100 nM). (C) Violin plots showing expression levels of genes critical for hematopoietic differentiation from HSC, MPP, MEP, MKP, platelet, mature myeloid, and erythroid lineage stages for all diabody conditions on day 12 in culture. (D) UMAP plots showing scRNA-seq data of FACS-isolated human HSCs ($CD34^+CD45RA^-CD90^+CD38^-$) after treatment with blocking antibodies against TPO (R&D, AF-288-NA). (E) Graphical schemata showing effects of diabodies on HSC proliferation and megakaryocytic differentiation.

Despite substantial efforts to identify factors in the microenvironment of the bone marrow to support HSC stemness (2, 3, 6, 7), it has not as yet been possible to stably expand purified human HSPCs ex vivo for clinical use despite preclinical work demonstrating that HSCs can be propagated in culture with polyvinyl alcohol (PVA) scaffold, pyrimidoindole-derived molecules, HOXB, or by suppressing the aryl hydrocarbon receptor (16, 42–44). In this study we demonstrated that partial agonistic DBs AK111 and AK113 allow for HSPC maintenance and expansion ex vivo by diminishing and/or modulating activating downstream signals through TPO-R. In contrast to these other approaches which act through obscure mechanisms, TPO DBs modulate signaling solely through the TPO-R; thus side effects are anticipated to be minimal. TPO-DBs are able to deliver customized intensities of downstream TPO-R signals, and thus mimic the physiological conditions of the TPO regulation while more tightly controlling downstream signaling output. In addition, the TPO DBs split the functions of TPO with regard to megakaryopoiesis and HSPC expansion, a unique feature, which is not a property of any of the available TPO mimetics nor the above-mentioned stem cell expanding experimental reagents. The dual function of TPO is an unanswered and burning open question in the otherwise well-studied field of TPO signaling. Thus, TPO DBs also represent an interesting reagent for further exploratory research in this area.

The importance of cytokines in maintaining the HSPC pool and cell lineage specifications has been well established in the literature. For instance, SCF and TPO are required cytokines for HSPCs. While HSPCs generated by DBs show strong gene expression similarities with uncultured HSPCs by single-cell RNA-seq, they also have very specific features. HSC_{AK111} expressed increased IL6R and decreased FLT3 ligand compared to uncultured HSPCs. It is understood that the expression of FLT3 increases between the HSPC and MPP stage and plays a key role for multipotent and lymphoid progenitors and myeloid cells. While the absence of FLT3L does not alter megakaryocyte-erythroid progenitor development, the cytokine TPO has been shown to potentiate FLT3-mediated effects. Our single-cell RNA-seq data show that HSPCs cultured with partial agonistic TPO DBs lacked FLT3 expression and retained at least short-term stem cell-like properties; thus, these culture conditions appear optimal for stem cell maintenance.

Using single-cell transcriptomics (scRNA-seq) in conjunction with protein expression studies, we confirmed that the stem cells generated by DBs produce an original pool of stem cells in vitro (45, 46). By clustering HSPCs and MPPs we can conclude that after nearly 2 wk of culture, the HSC_{AK111} populations are closer to HSPC than MPP populations. For example, the HSC_{AK111} populations demonstrate a TP53 expression pattern very similar to that of uncultured HSPCs. We know that TP53 expression is tightly controlled in HSPCs, and it has been shown that the Trp53, p16, p19 triple mutant allows long-term hematopoietic reconstitution (47) and HSPC expansion (48). Our studies show a basal low level of TP53 in HSC AK111 quite similar to HSCs.

More recently, it has been demonstrated that mutations in the cytokine TPO reduce engraftment capacity, further demonstrating the essential role of TPO for primary hematopoiesis (42, 49). The use of TPO as a drug initially had been quite limited due to antibody formation and thrombocytopenia. Nevertheless,

the second generation of TPO receptor agonists are now being used successfully in the clinic for severe immune thrombocytopenias and bone marrow failure syndromes and are under evaluation for a wide range of other thrombocytopenic disorders, including those associated with chemotherapy and myelodysplastic syndromes. Thus, while generally much better tolerated, unwanted side effects still occur with second generation TPO mimetics, including thrombocytosis, thrombosis, bone marrow reticulosis, rebound thrombocytopenia, and liver toxicity. DBs deliver different intensities of downstream MPL signals, and thus mimic the physiological conditions of TPO regulation while more tightly controlling downstream signaling output. In addition to the above-discussed applications, we found this to be particularly relevant to oncogenic signaling downstream of the TPO-R as they occur in ET, a myeloproliferative neoplasm. To our great surprise we discovered that partial agonistic TPO DB blocked oncogenic colony formation in patients with ET by partially agonizing downstream signaling of TPO-R. Potential clinical applications of TPO DB could be conditions requiring full or partial TPO agonism such as platelet production, HSC expansion/maintenance, as well as oncogenic signaling in ET.

Materials and Methods

Details of the experimental protocols can be found in *SI Appendix, Supplementary Materials and Methods*.

TPO-R Diabodies Binding Experiments. The *Saccharomyces cerevisiae* strain EBY100 was transformed with the pCT302_TPO-R SD1-2 vector and grown for 2 d at 30 °C on selective dextrose casamino acids (SDCAA) media, followed by induction in selective galactose casamino acids (SGCAA) media (pH 4.5) for 2 d at 20 °C. Yeast were then incubated with the indicated concentrations of biotinylated TPO-R diabodies for 1 h at 4 °C, followed by streptavidin-Alexa 647 (1:200 dilution) for 15 min at 4 °C. Fluorescence was analyzed on an Accuri C6 flow cytometer.

Statistics. Statistical analyses were performed using Prism software (GraphPad Software). Statistical significance was determined by the unpaired Student's *t* test for comparisons between two groups and one-way ANOVA for multigroup comparisons (ns, nonsignificant; $P > 0.05$; $*P < 0.05$; $**P < 0.01$; $***P < 0.001$; $****P < 0.0001$). In statistical graphs, points indicate individual samples, and results represent the mean \pm SD unless indicated otherwise.

Study Approval. Healthy deidentified human bone marrow samples were acquired from AllCells. Essential thrombocytosis bone marrow samples were deidentified and acquired from the Stanford University Medical Center through Jason Gotlib, according to Institutional Review Board (IRB)-approved protocol 18329 or as discard samples from the Pathology Department under IRB 39881. Mice were maintained in the Stanford University Laboratory Animal Facility in accordance with Stanford Animal Care and Use Committee and National Institutes of Health guidelines (SU-APLAC 30912).

Data Availability. scRNA sequencing data have been deposited in the Gene Expression Omnibus (GEO) at the National Center for Biotechnology Information (NCBI) under accession [GSE115235](https://www.ncbi.nlm.nih.gov/geo/query/acc.cgi?acc=GSE115235). All the data are included in the main text and supporting information.

ACKNOWLEDGMENTS. K.C.G. acknowledges NIH-RO1-AI51321, the Ludwig Institute, the Mathers Foundation, and HHMI for funding; G.W. acknowledges the National Heart, Lung, and Blood Institute, the Ludwig Institute, Scleroderma Research Foundation (SRF), and the Emerson Collective. Deutsche Forschungsgesellschaft (DFG) provided salary support to T.L. and I.S.H. was supported by Cancer Research UK grant A24593 and by the University of York Technology Facility.

1. S. Lok et al., Cloning and expression of murine thrombopoietin cDNA and stimulation of platelet production in vivo. *Nature* **369**, 565–568 (1994).
2. F. Wendling et al., cMpl ligand is a humoral regulator of megakaryocytopoiesis. *Nature* **369**, 571–574 (1994).
3. F. J. de Sauvage et al., Stimulation of megakaryocytopoiesis and thrombopoiesis by the c-Mpl ligand. *Nature* **369**, 533–538 (1994).
4. K. Kaushansky et al., Promotion of megakaryocyte progenitor expansion and differentiation by the c-Mpl ligand thrombopoietin. *Nature* **369**, 568–571 (1994).

5. I. Vigon et al., Molecular cloning and characterization of MPL, the human homolog of the v-mpl oncogene: Identification of a member of the hematopoietic growth factor receptor superfamily. *Proc. Natl. Acad. Sci. U.S.A.* **89**, 5640–5644 (1992).
6. I. Vigon et al., Characterization of the murine Mpl proto-oncogene, a member of the hematopoietic cytokine receptor family: Molecular cloning, chromosomal location and evidence for a function in cell growth. *Oncogene* **8**, 2607–2615 (1993).
7. R. C. Skoda et al., Murine c-mpl: A member of the hematopoietic growth factor receptor superfamily that transduces a proliferative signal. *EMBO J.* **12**, 2645–2653 (1993).

8. A. L. Gurney, K. Carver-Moore, F. J. de Sauvage, M. W. Moore, Thrombocytopenia in c-mpl-deficient mice. *Science* **265**, 1445–1447 (1994).
9. F. J. de Sauvage *et al.*, Physiological regulation of early and late stages of megakaryocytopoiesis by thrombopoietin. *J. Exp. Med.* **183**, 651–656 (1996).
10. H. Yoshihara *et al.*, Thrombopoietin/MPL signaling regulates hematopoietic stem cell quiescence and interaction with the osteoblastic niche. *Cell Stem Cell* **1**, 685–697 (2007).
11. H. Qian *et al.*, Critical role of thrombopoietin in maintaining adult quiescent hematopoietic stem cells. *Cell Stem Cell* **1**, 671–684 (2007).
12. S. Kimura, A. W. Roberts, D. Metcalf, W. S. Alexander, Hematopoietic stem cell deficiencies in mice lacking c-Mpl, the receptor for thrombopoietin. *Proc. Natl. Acad. Sci. U.S.A.* **95**, 1195–1200 (1998).
13. G. P. Solar *et al.*, Role of c-mpl in early hematopoiesis. *Blood* **92**, 4–10 (1998).
14. K. Carver-Moore *et al.*, Low levels of erythroid and myeloid progenitors in thrombopoietin-and c-mpl-deficient mice. *Blood* **88**, 803–808 (1996).
15. N. Fox, G. Priestley, T. Papayannopoulou, K. Kaushansky, Thrombopoietin expands hematopoietic stem cells after transplantation. *J. Clin. Invest.* **110**, 389–394 (2002).
16. A. C. Wilkinson *et al.*, Long-term ex vivo haematopoietic-stem-cell expansion allows nonconditioned transplantation. *Nature* **571**, 117–121 (2019).
17. Y. Pikman *et al.*, MPLW515L is a novel somatic activating mutation in myelofibrosis with myeloid metaplasia. *PLoS Med.* **3**, e270 (2006).
18. A. D. Pardanani *et al.*, MPLS15 mutations in myeloproliferative and other myeloid disorders: A study of 1182 patients. *Blood* **108**, 3472–3476 (2006).
19. M. Ballmaier *et al.*, c-mpl mutations are the cause of congenital amegakaryocytic thrombocytopenia. *Blood* **97**, 139–146 (2001).
20. A. Pecci *et al.*, Thrombopoietin mutation in congenital amegakaryocytic thrombocytopenia treatable with romiplostim. *EMBO Mol. Med.* **10**, 63–75 (2018).
21. D. M. Townsley *et al.*, Eltrombopag added to standard immunosuppression for aplastic anemia. *N. Engl. J. Med.* **376**, 1540–1550 (2017).
22. D. J. Kuter, Clinical applications of thrombopoietic growth factors. <https://www.upToDate.com/contents/clinical-applications-of-thrombopoietic-growth-factors>. Accessed 4 January 2018.
23. J. B. Bussel *et al.*, Eltrombopag for the treatment of chronic idiopathic thrombocytopenic purpura. *N. Engl. J. Med.* **357**, 2237–2247 (2007).
24. W. Vainchenker, I. Plo, C. Marty, L. N. Varghese, S. N. Constantinescu, The role of the thrombopoietin receptor MPL in myeloproliferative neoplasms: Recent findings and potential therapeutic applications. *Expert Rev. Hematol.* **12**, 437–448 (2019).
25. L. N. Varghese, J. P. Defour, C. Pecquet, S. N. Constantinescu, The thrombopoietin receptor: Structural basis of traffic and activation by ligand, mutations, agonists, and mutated calreticulin. *Front. Endocrinol. (Lausanne)* **8**, 59 (2017).
26. S. Wilmes *et al.*, Mechanism of homodimeric cytokine receptor activation and dysregulation by oncogenic mutations. *Science* **367**, 643–652 (2020).
27. J. Staerk *et al.*, Orientation-specific signalling by thrombopoietin receptor dimers. *EMBO J.* **30**, 4398–4413 (2011).
28. J. Li *et al.*, Thrombocytopenia caused by the development of antibodies to thrombopoietin. *Blood* **98**, 3241–3248 (2001).
29. K. Nakano *et al.*, Effective screening method of agonistic diabodies based on autocrine growth. *J. Immunol. Methods* **347**, 31–35 (2009).
30. I. Moraga *et al.*, Tuning cytokine receptor signaling by re-orienting dimer geometry with surrogate ligands. *Cell* **160**, 1196–1208 (2015).
31. C. Gawad, W. Koh, S. R. Quake, Single-cell genome sequencing: Current state of the science. *Nat. Rev. Genet.* **17**, 175–188 (2016).
32. Tarashansky A. J., Yuan X., S. R. Quake, B. Wang, Self-assembling manifolds in single-cell RNA sequencing data. *Elife* **8**, e48994 (2018).
33. S. Nikiforow, J. Ritz, Dramatic expansion of HSCs: New possibilities for HSC transplants? *Cell Stem Cell* **18**, 10–12 (2016).
34. V. Sangkhoe, S. J. Saur, A. Kaushansky, K. Kaushansky, I. S. Hitchcock, Phosphorylated c-Mpl tyrosine 591 regulates thrombopoietin-induced signaling. *Exp. Hematol.* **42**, 477–486.e4 (2014).
35. G. A. Millot, W. Vainchenker, D. Duménil, F. Svinarchuk, Distinct effects of thrombopoietin depending on a threshold level of activated Mpl in BaF-3 cells. *J. Cell Sci.* **115**, 2329–2337 (2002).
36. Y. Royer, J. Staerk, M. Costuleanu, P. J. Courtoy, S. N. Constantinescu, Janus kinases affect thrombopoietin receptor cell surface localization and stability. *J. Biol. Chem.* **280**, 27251–27261 (2005).
37. L. Papa *et al.*, Ex vivo human HSC expansion requires coordination of cellular reprogramming with mitochondrial remodeling and p53 activation. *Blood Adv.* **2**, 2766–2779 (2018).
38. K. Mohan *et al.*, Topological control of cytokine receptor signaling induces differential effects in hematopoiesis. *Science* **364**, eaav7532 (2019).
39. J. L. Mendoza *et al.*, Structure of the IFN γ receptor complex guides design of biased agonists. *Nature* **567**, 56–60 (2019).
40. S. Mitra *et al.*, Interleukin-2 activity can be fine tuned with engineered receptor signaling clamps. *Immunity* **42**, 826–838 (2015).
41. C. C. M. Ho *et al.*, Decoupling the functional pleiotropy of stem cell factor by tuning c-kit signaling. *Cell* **168**, 1041–1052.e18 (2017).
42. S. Kohlscheen, F. Schenk, M. G. E. Rommel, K. Cullmann, U. Modlich, Endothelial protein C receptor supports hematopoietic stem cell engraftment and expansion in Mpl-deficient mice. *Blood* **133**, 1465–1478 (2019).
43. I. Fares *et al.*, Pyrimidoindole derivatives are agonists of human hematopoietic stem cell self-renewal. *Science*, 10.1126/science.1256337 (2014).
44. E. Csaszar, Rapid expansion of human hematopoietic stem cells by automated control of inhibitory feedback signaling. *Cell Stem Cell*, 10.1016/j.stem.2012.01.003 (2012).
45. S. Nestorowa *et al.*, A single-cell resolution map of mouse hematopoietic stem and progenitor cell differentiation. *Blood* **128**, e20–e31 (2016).
46. X. T. Huang *et al.*, Technical advances in single-cell RNA sequencing and applications in normal and malignant hematopoiesis. *Front. Oncol.* **8**, 582 (2018).
47. O. O. Akala *et al.*, Long-term haematopoietic reconstitution by Trp53 $^{-/-}$ p16Ink4a $^{-/-}$ p19Arf $^{-/-}$ multipotent progenitors. *Nature* **453**, 228–232 (2008).
48. M. TeKippe, D. E. Harrison, J. Chen, Expansion of hematopoietic stem cell phenotype and activity in Trp53-null mice. *Exp. Hematol.* **31**, 521–527 (2003).
49. A. Seo *et al.*, Bone marrow failure unresponsive to bone marrow transplant is caused by mutations in *thrombopoietin*. *Blood* **130**, 875–880 (2017).